Rupture kinematics and strong ground motion estimates of the 2005, Mw 8.6, Nias- Simeulue earthquake from the joint inversion of seismic and geodetic data

A. Ozgun Konca, Vala Hjorleifsdottir, Don V. Helmberger, Kerry Sieh, Jean-Philippe Avouac, Richard Briggs, Aron Meltzner, Alex Song, John Galetzka, Danny Hilman Natawidjaja, Bambang Suwargadi, Yehuda Bock and Linette Prawirodirdjo

1. Mw 8.6 Nias Earthquake

The seismic sources, near-field ground deformations and strong-motion generation of large subduction earthquakes remain poorly known.

The 2005, Mw 8.6, Nias-Simeulue earthquake was caused by rupture of a portion of the Sunda megathrust offshore northern Sumatra. This earthquake occurred within an array of continuous GPS stations and produced measurable vertical displacement of the fringing coral reefs above the fault rupture.

The geodetic constraints on slip distribution eliminate the trade-off between the slip and rise time inherent to purely seismic inversions. This enables better estimates of the temporal evolution of rupture and strong ground motion estimates.

Thus, the Nias-Simeulue earthquake provides a unique opportunity to assess the source characteristics and the generation of strong ground motions due to a megathrust event from the joint analysis of teleseismic waveforms and near-field static displacements.

2. Data

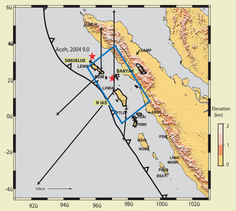

Figure 1A: coseismic GPS data

the Sumatran GPS Array (SuGAr), had been deployed in the years and months preceding the earthquake by Caltech Tectonic Observatory. The stations record at a 120-second sampling rate (data avaiable at http://www.tectonics.caltech.edu/sumatra/data).

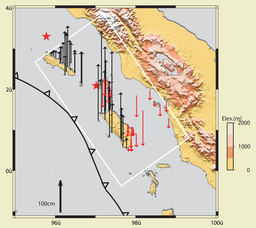

Figure 1B: coral uplift and subsidence data

The second geodetic dataset comes from field measurements of coseismic uplift and subsidence (Briggs et al., 2005) utilizing porites coral microatolls, which act as natural recorders of sea level changes with accuracies of a few centimeters

Figure 1C: seismic stations used in the inversion

The teleseismic waveforms were selected from the IRIS network. The broadband seismograms were bandpass filtered from 0.8 s (P-waves) and 2 s (SH-waves) to 200 s.

3. Models using combinatinations of datasets

Since three different datasets are included into the inversion, we tested various solutions and combinations to understand the constraints provided by each particular dataset. The model obtained from the inversion of only the seismic data yields a misfit of 15%. The fit to the waveforms is indeed quite good. By contrast, this model provides a very poor fit to the geodetic data (Figure 4A), while models utilizing geodetic data fits very well . The misfit to the waveforms does not vary much when the geodetic data are taken into account and remains in the 15%-20% range .

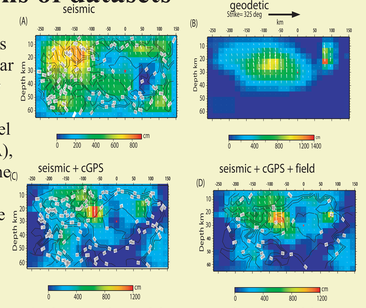

Figure 2: slip maps for models using combinations of datasets

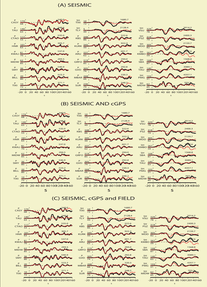

Figure 3: waveform fits

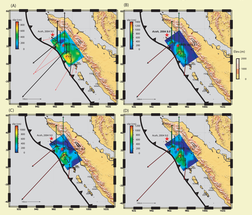

Figure 4: geodetic fits

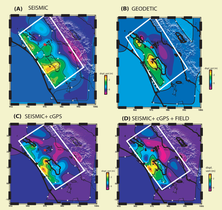

Figure 5: waveform fits

4. Rupture velocity and rise time

The rise time and rupture velocity are fundamental earthquake parameters and they are critical in terms of estimating near-field motions. In order to find these kinematic parameters, we have tested various rupture velocities where the rise times are characterized by cosine functions for each box. Rise times are set to vary between 2 to32s . Even with the limited number of model parameters for the rise time, we still can fit the waveform data quite well for different fixed rupture velocities, as displayed in Figure 6.

Note that the largest slip patch, south of the hypocenter, shows a direct trade-off between the rupture velocity and rise time. In the model with Vr = 2 km/s, the width of the rise times S(t) are mostly between 10 s and 20 s, whereas in the model with Vr=3km/s, rise times are mostly ~25s or greater. The fits to the geodetic data and seismic waveforms are slightly better for the case where rupture velocity is fixed to 2 km/s compared to the cases where it is fixed to some higher value (Table 1). This improvement might be insignificant; however, considering the trend in the misfits moving from rupture velocity of 3 km/s to 2 km/s, the model with the rupture velocity of 2 km/s might be preferable.

Dataset	Vr (km/s)	Rise time (s)	Moment Magn.	Waveform misfit	Geodetic chi-sq misfit(χ^2)	Misfit of cGPS(cm)**	Misfit to the coral(cm)	Total misfit to geodetic(cm)
Seismic	1-3	2-32	8.8	15 %	12923	38.22	99.00	38.28
Seismic	2	2-32	8.67	17%	12357	37.36	99.24	37.43
Seismic	3	2-32	8.43	19%	12333	37.33	99.24	37.38
cGPS & corals	---	---	8.59	---	14.63	1.02	35.46	1.29
Seismic & cGPS	1-3	2-32	8.64	16.4%	41.19	1.28	61.50	1.87
Seismic & cGPS & corals	1-3	2-32	8.64	16.5%	15.85	1.17	29.75	1.34
Seismic & cGPS & corals	2	2-32	8.61	18.5%	14.98	1.10	31.38	1.30
Seismic & cGPS & corals	2.4	2-32	8.59	19.7%	15.6	1.08	34.60	1.33
Seismic & cGPS & corals	3	2-32	8.54	21.3%	18.18	1.17	37.31	1.44
Seismic & cGPS & corals	1-3	10	8.64	16.9%	18.44	1.17	38.56	1.45
Seismic & cGPS & corals	1-3	30	8.69	19%	19.8	1.37	27.04	1.50

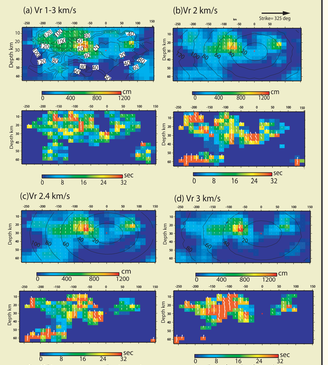

Figure 6: Slip map and rise time map on the fault for (A) variable rupture velocity (B) Vr = 2 km/s (C) Vr = 2.4 km/s (D) Vr = 3 km/s. Rise times are shown for the subfaults that slip more then 2 meters, since the ones that slip less can not be constrained reliably.

Table 1: The moments, waveform and geodetic misfits listed for the various solutions. The waveform misfits are a combination of L1 and L2 norms (Ji et al., 2002). The geodetic misfits are sum-squared residuals.

5. testing models against surface waves

In spite of the constraints provided by the geodetic data, there are still some trade-offs among the model parameters. Here we use long period surface waves to test these models.

In the source inversions, the trade-off between the rupture velocity and rise time depends on the apparent velocity of the modeled phase. As the models with different kinematic parameters were made to fit the P and S-waves, there will be a phase shift of the Rayleigh waves depending on the rupture velocity. Using the least average time shift as a criterion leads us to estimate the rupture velocity for the Nias-Simeulue event to be around 2.-2.5 km/s.

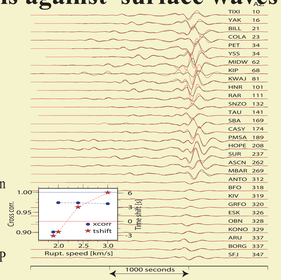

Figure 7: The 100s-500s waveform fits computed using a 3D Spectral Element Method for the model with fixed rupture velocity of 2.4 km/s. The seismograms are 30-100 degree distance and are sorted by azimuth and aligned on the Rayleigh wave (3.8 km/s phase velocity). The inset shows the average cross correlations (blue circles) and time shifts (red stars). The variable rupture velocity is plotted at 1.9 km/s.

6. strong-motion estimates

Figure 9: The estimated time evolution of ground displacement and velocity at the station Lahewa (LHWA), Nias Island, for various inversions. (A) Predictions for seismic and joint inversions for varying rupture velocity (B) predictions for joint inversions for fixed rupture velocities of 2, 2.4 and 3 km/s and fixed rise times of 10s and 30s.

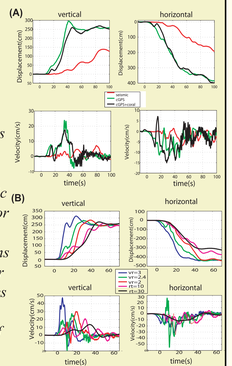

7. conlusions and future work

Despite the significant trade-offs between rise time and rupture velocity, the slip pattern of the Nias-Simeulue event is quite well determined, due to the unique abundance of geodetic data above the source region. Our analysis implies that the earthquake was caused by the rupture of two asperities. A big patch under northern and central Nias island, with maximum slip of about 12 m, a smaller patch under southern Simuelue island, and a slip gap between the two islands are common features of all our joint inversions.

We estimate kinematic parameters by minimizing the time shift in the long-period seismograms and misfit to the dataset used in the inversion. We favor an average rupture velocity of 2 to 2.5 km/s. If this is correct, then the rupture velocity is only 50-60 % of the shear wave speed of the 1D model, far lower than rupture velocities seen during the Chi-Chi and Tokachi-oki earthquakes, for which rupture velocity was typically about 80-90 % of the shear wave speed.

Our modeling yields rise times for the Nias-Simeulue earthquake between 10-15 seconds, which is similar to other large subduction zone earthquakes.

Models used in this study disagree with the normal mode data. This implies that either the dip or the moment is wrong constraint used n the modeling is . Our preliminary attempts show that dip of 8 degrees might be more suitable for the Nias earthquake rather than 15 degrees used in this inversion. The next step is to find a better geometry to satisfy the mode data.